Spectroscopic Studies of Soft X-Ray Emission from Gadolinium Plasmas

I. Kambali* **and G. O'Sullivan**
School of Physics, University College Dublin, Ireland

ARTICLE INFO

Article history:
Received 8 November 2013
Received in revised form 9 May 2014
Accepted 9 May 2014

Keywords:
Spectroscopy
Laser-produced plasmas
Soft X-ray emission
Unresolved-Transition Arrays (UTA)
Atomic spectra

ABSTRACT

The temporal behavior of gadolinium (Gd) laser-produced plasmas has been studied using a modified grazing incidence spectrometer which allows to capture the evolution of the plasma with spectral and temporal resolution of 0.1 nm and 1 ns, respectively. Experimental results indicate that the soft X-ray emission follows the temporal behavior of the laser pulse at high laser power density of $\Phi = 4.4\times10^{12}$ W/cm^2 in which the soft X-ray emission lasts for 7.5 ns (at FWHM) whereas at $\Phi = 5.4\times10^{11}$ W/cm^2 and $\Phi = 7.6\times10^{10}$ W/cm^2 the emission lasts for only 4 ns and 2.5 ns respectively, these are shorter than laser pulse duration due to lower electron temperatures achieved in the plasma generation. Lower Gd ion stages ranging from Gd^{11+} – Gd^{14+} are also found to contribute to the spectral emission over time.

INTRODUCTION

Soft X-ray sources based on rare-earth elements such as gadolinium (Gd) and terbium (Tb) below 13.5 nm have been of great interest and are still a subject of ongoing research both theoretical and experimental [1–4]. The feasibility of Gd and Tb for next generation photolithography in semiconductor industries has been highlighted by a joint group of researchers from the Institute for Spectroscopy of Russian Academy of Sciences (ISAN) and ASML of the Netherlands [5,6] who also proposed the target materials as potential soft X-ray sources around 6.5 – 6.7 nm due to the availability of Mo/B_4C and other multilayer mirrors with a theoretical reflectivity of up to 80% around these wavelengths [7]. The unresolved-transition array (UTA) which is responsible for the strong X-ray emission around this wavelength has been previously identified by Churilov and co-workers [8], and again is due to primarily from 4p – 4d and 4d – 4f transitions.

Recent work on Gd laser-produced plasma (LPP) has been focused on the spectral behavior of the UTA over different power densities, initial target densities and conversion efficiencies (CE) [9-12]. Experimental work has proven that high power density [11], hence high electron temperatures, are required to create high ion stages of Gd (especially Ag- and Pd-like Gd XVIII – Gd XXI) [13] for effectively generating intense soft X-ray emission around 6.7 nm. In addition, a plasma temperature around 110 eV is needed for optimum brightness at 6.76 nm [13-16].

A study of the dependence of CE on laser wavelength revealed that a sub-nanosecond laser pulse would be required to optimize the generation of X-ray from Gd targets [11], though the in-band CE obtained from this experiment was only 0.4% (into a 0.6% bandwidth), and it was also suggested that the use of a laser with a longer wavelength such as CO_2 would be expected to produce a higher CE. Nevertheless, a CE greater than 1% has been demonstrated (into a 2% bandwidth) in the laboratory with a Nd:YAG laser operating at λ = 1064 nm for a pure Gd target whereas a higher CE was achieved with a Gd_2O_3 target even though self-absorption at the peak emission remains a big issue in both target materials [10]. As reported in the tin case [17], X-ray emission from a Gd LPP is expected to largely depend upon the viewing angle of the captured emission, and this hypothesis has been experimentally confirmed by O'Gorman and co-workers [12] in which spectra observed at a 90^o-viewing angle showed more pronounced self-absorption than at 45^o and was predominantly due to lower ion stages of Gd that, based on previous theoretical calculations for Sn LPP [18], result from cold plasma produced by the soft X-ray emission it self on the target surface surrounding the plasma.

The temporal evolution of soft X-ray spectra is also of great interest particularly to understand the behavior of the X-ray emission over time. In this

* Corresponding author.
E-mail address: imam.kambali@ucdconnect.ie

paper the latest experimental studies on the time-resolved spectroscopy of Gd LPPs are reported.

EXPERIMENTAL METHODS

A surelite Nd:YAG laser operating at 1064 nm, 10 Hz repetition rate and 7 ns duration (at Full Width at Half Maximum = FWHM) delivering photon energy of up to 530 mJ was directed onto a pure Gd foil target (99.99% purity, 1 mm thick). The soft X-ray spectra were captured by an ultra high speed gated Hamamatsu ICCD camera (type C-7164-03) mounted in a modified ISAN spectrometer which covers the wavelength range from 5 – 10 nm. The Gd target was irradiated with only 2 shots at each time delay whereas spectra from an Al target were used for wavelength calibration.

The intense unresolved transition arrays (UTA) responsible for the soft x-ray emission around 6.7 nm were calculated by the Cowan suite of codes [19] which can be seen in Fig. 1.

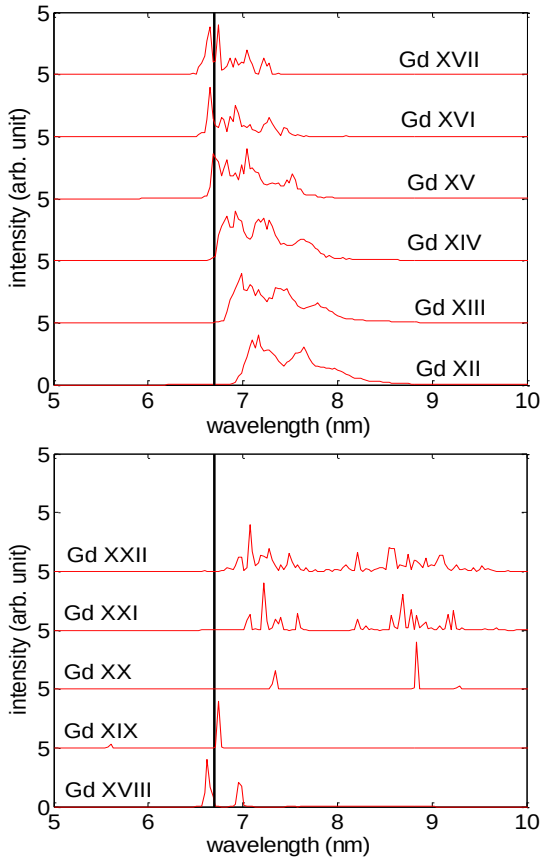

Fig. 1. Gadolinium spectra (Gd XII – Gd XXII) calculated by the Cowan suite of codes convolved with Gaussian broadening of 0.03 nm. The 1% bandwidth for 6.7 nm wavelength is highlighted with the dark vertical lines.

The transitions involved in the gadolinium spectra calculations were the resonance $4d^{10}4f^{n} – 4d^{9}4f^{n+1}$ + $4d^{10}4f^{n-1}(5d,5g)$ + $4d^{9}4f^{n}(5p,5f)$ (for Gd XII – Gd XVIII), – $4p^{6}4d^{9}(nl)$ + $4p^{5}4d^{10}5s$ (for Gd XIX) and $4p^{6}4d^{n} – 4p^{6}4d^{n-1}(nl)$ + $4p^{5}4d^{n+1}$ + $4p^{5}4d^{n}5s$ (for Gd XX – Gd XXII). The figure clearly indicates that the X-ray emission from lower and higher ion stages of Gd ranging from Gd XII – Gd XIII and Gd XX – Gd XXII occurs at longer wavelengths whereas Gd XIV – Gd XIX are more likely to become the candidates which emit strong radiation around the wavelength of interest.

These calculated results agree with the earlier theoretical and experimental results using laser-produced as well as vacuum spark plasmas reported by Churilov *et al.* [13]. They suggested that the strong emission in the 6.5 – 7.5 nm region resulted from the $4d^{10}4f^{n} – 4d^{9}4f^{n+1}$ transitions in the ion stages with a partially filled 4f shell. They also highlighted that the most intense emission around 6.7 nm was predicted to be due to $4d^{10}4f^{2} – 4d^{9}4f5d$ transition in Gd XVII. This means that high laser power density is required to sufficiently generate EUV radiation around 6.7 nm. The power density ranges have been identified by O'Sullivan and co-workers [14] which highlights that for Nd:YAG lasers (λ = 1.06 nm) one will need to employ a laser irradiance between $2\times10^{12} – 10^{13}$ W/cm^2 whereas for CO_2 laser (λ = 10.6 nm) the required power density is between $2\times10^{11} – 10^{12}$ W/cm^2.

RESULTS AND DISCUSSION

Temporal evolution of Gd spectra

The time-resolved spectra of Gd LPPs (recorded at 2 ns exposure time) were experimentally studied at 3 different power densities by changing the laser spot sizes while keeping laser energy fixed at 530 mJ, resulting in power densities of $\Phi = 7.6\times10^{10}$ W/cm^2 (laser spot diameter of 360 μm), $\Phi = 5.4\times10^{11}$ W/cm^2 (laser spot diameter of 130 μm), and $\Phi = 4.4\times10^{12}$ W/cm^2 (laser spot diameter of 50 μm).

At $\Phi = 7.6\times10^{10}$ W/cm^2 ((laser spot diameter of 360 μm, (Fig. 2(a)), the plasma starts to emit significant EUV radiation at t = –4 ns (4 ns before the EUV peak emission) which is dominated by emission around 6.9 nm and a feature around 7.4 nm which are both associated with emission from $Gd^{9+} – Gd^{13+}$ (according to the Cowan calculations and also as discussed in reference [1] at this relatively low irradiance). Note that all of the spectra were timed with respect to the peak emission at $\Phi = 4.4\times10^{12}$ W/cm^2. The shape of the spectrum does not change much with time because at this power density the plasma is not hot enough to

produce higher ion stages and therefore the emission ratio between the two peaks remains almost constant, though they broaden around the peak of the emission (at t = 0 ns). The continuum radiation due to most likely recombination is also relatively high particularly near the peak of the emission.

At Φ = 5.4×10^{11} W/cm^2 (Fig. 2(b)), there are significant differences in the spectral shape over time particularly in the peak emission which shifts to around 6.7 nm. In the early stages of the plasma (t = –5 to –2 ns), the EUV spectral shape is quite flat over the wavelength range of 6.6 – 7.3 nm which indicates that lower stage Gd ions predominate. Only 1 ns before the peak of the emission, the UTA around 6.7 nm gradually increases even though there are some pronounced dips near 6.9 nm (particularly at t = –2 ns and t = 2 ns, presumably from Gd^{13+} and Gd^{14+}) as well as at 7.5 nm (mainly due to Gd^{11+} – Gd^{12+}) which indicate the presence of self-absorption from lower ion stages of Gd, as also widely observed in Sn targets [17]. At this laser power density the self-absorption is present at all times and also is confirmed by the time-integrated spectra (Fig. 2(d)). The most dramatic changes in the spectral shape occur at the peak of the EUV emission where the 6.7 nm emission is a lot brighter than the rest of the wavelength range covered by the modified ISAN spectrometer. However the emission very quickly decreases as the temperature drops essentially following the laser temporal profile.

At a laser irradiance Φ = 4.4×10^{12} W/cm^2, which is high enough to get Pd- and Ag-like Gd stages, the shape of the spectra also changes significantly which shows the domination of the peak around 6.7 nm over the course of the X-ray emission (Fig. 2(c)). The in-band intensity around 6.7 nm at this power density is nearly 2.5 times higher than that of when the Gd target is illuminated with Φ = 5.4×10^{11} W/cm^2 (or almost 10 times higher than that when the target is irradiated with Φ = 7.6×10^{10} W/cm^2). This behavior is primarily due to higher electron temperatures throughout the entire plasma life time at this power density which is high enough to further ionize Gd atoms compared to the lower power densities. Nevertheless some self-absorption by lower ion stages of Gd is also obvious at the higher power density, though they are less pronounced than at lower power density. As well, from the time-integrated spectra (Fig. 2(d)) one can directly see the dependence of Gd spectral shape on the laser power density in which the in-band intensity at 6.7 nm reaches its highest intensity when the target is irradiated at Φ = 4.4×10^{12} W/cm^2.

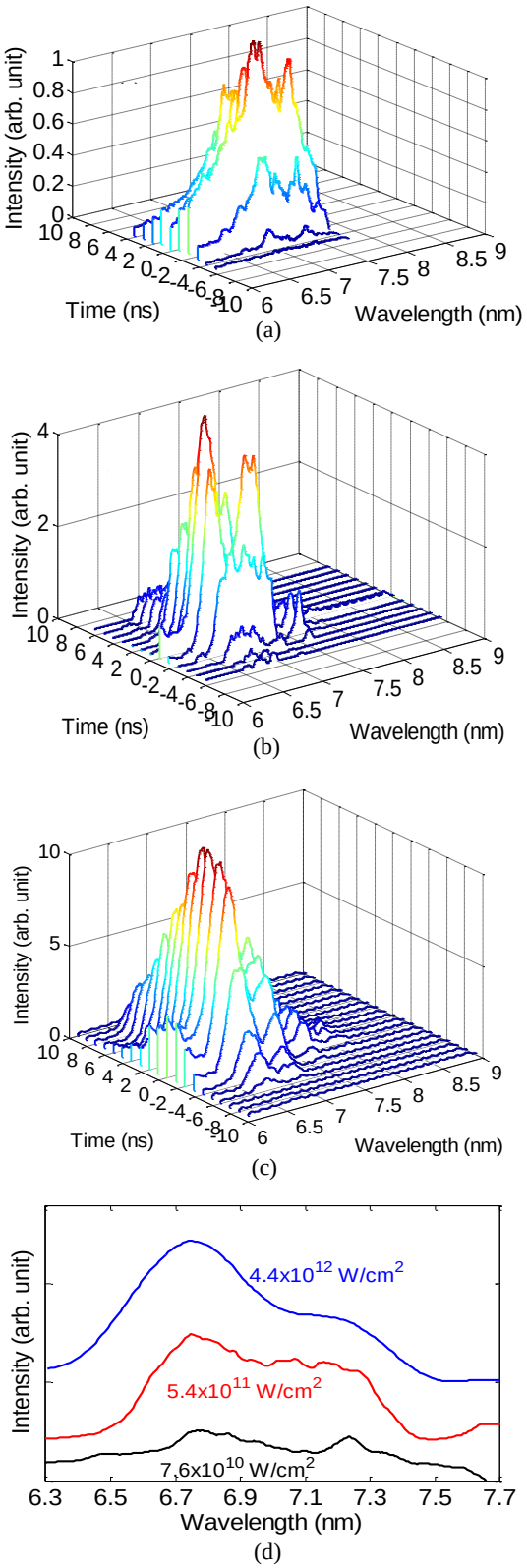

Fig. 2. Temporal evolution of Gd spectra at (a) Φ = 7.6×10^{10} W/cm^2 (laser spot diameter of 360 μm), (b) Φ = 5.4×10^{11} W/cm^2 (laser spot diameter of 130 μm), and (c) Φ = 4.4×10^{12} W/cm^2 (laser spot diameter of 50 μm). The time-integrated spectra for different laser power densities is shown in (d).

Lower ion stages contributions and the in-band intensities

The contributions of lower Gd ion stages ranging from Gd^{11+} – Gd^{14+} was also analyzed for the investigated laser irradiance as shown in Fig. 3(a) – (c) in which the integrated intensities of the wavelength regions dominated by Gd XII – Gd XV emission were normalized with respect to that associated with the maximum Gd XV intensity at each power density.

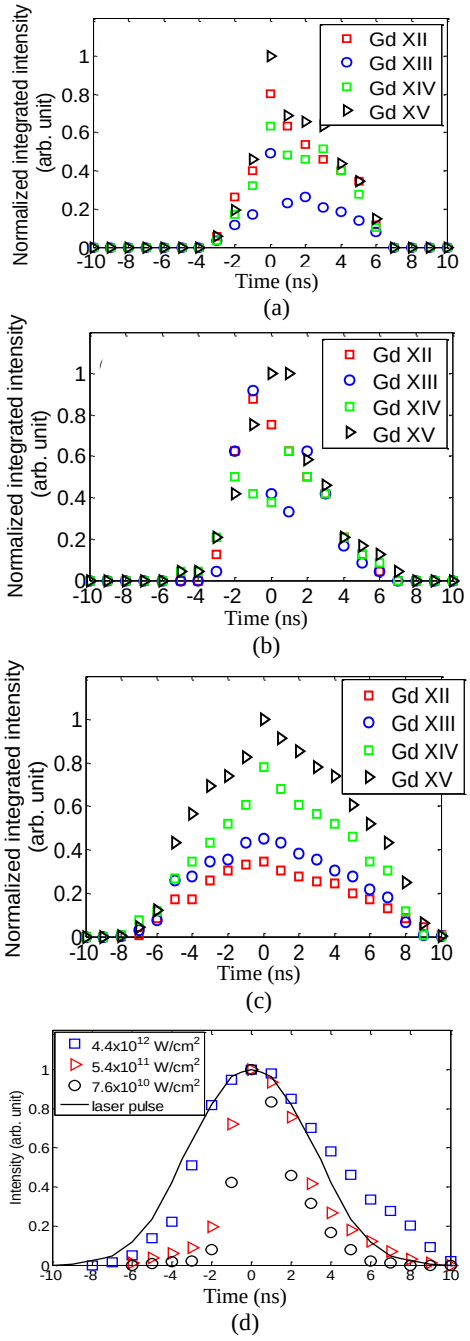

Fig. 3. Temporal evolution of the integrated intensities of the wavelength regions dominated by Gd XII to Gd XV for (a) Φ = 7.6×10^{10} W/cm^2, (b) Φ = 5.4×10^{11} W/cm^2, and (c) Φ = 4.4×10^{12} W/cm^2. The In-band X-ray intensity (at 6.7 nm ± 1% bandwidth) from Gd LPP corresponding laser fluxes are shown in (d).

Note that based on the Cowan code calculations [19] and earlier studies reported by Churilov *et al.* [1], the wavelength regions dominated by Gd^{11+}, Gd^{12+}, Gd^{13+}, Gd^{14+} are 7.1 – 7.4 nm, 6.9 – 7.1 nm, 6.8 – 6.9 nm and 6.75 – 6.8 nm, respectively.

At Φ = 7.6×10^{10} W/cm^2 the populations of Gd^{11+} – Gd^{13+} at the peak emission are relatively very high (their respective emission is nearly 80%, 50% and 60% of the Gd XV intensity). The lower ion stage contributions are still very high at the higher laser intensity of Φ = 5.4×10^{11} W/cm^2 which results in less effective emission near 6.7 nm. Increasing the laser power density to Φ = 4.4×10^{12} W/cm^2 eventually gives a dramatic decrease in the lower ion stage contributions, and therefore gives rise to the emission at the wavelength of interest.

While the absolute timing between the laser and the soft X-ray emission cannot be determined precisely in our experimental set up, we can plot the temporal profile of the laser and compare it with the in-band X-ray emission at 6.7 nm ± 1% bandwidth as shown in Fig. 3(d). Note that all of the spectra were timed with respect to the peak emission at Φ = 4.4×10^{12} W/cm^2. It is clear that the Gd plasma emits at over half its maximum intensity for approximately 2.5 ns at Φ = 7.6×10^{10} W/cm^2, 4 ns at Φ = 5.4×10^{11} W/cm^2 and 7.5 ns when the power density is increased to Φ = 4.4×10^{12} W/cm^2 and that the temporal behavior of the Gd EUV emission matches the temporal profile of the Nd:YAG laser at the later laser irradiance. The shorter plasma duration for lower power densities can be explained by the fact that the electron temperature must be above 100 eV to ionize Gd atoms to produce UTA responsible for the X-ray emission around 6.7, and this temperature is only reached at the temporal peak of the laser pulse [14,16].

CONCLUSION

We have studied the temporal behavior of gadolinium (Gd) laser-produced plasmas using a modified ISAN spectrometer between 5 nm and 15 nm, which allows us to capture the evolution of the plasma with spectral and temporal resolutions of 0.1 nm and 1 ns, respectively. We found that the EUV emission follows the temporal behavior of the laser pulse at the highest laser power density of Φ = 4.4×10^{12} W/cm^2 in which the soft X-ray emission lasts for 7.5 ns (at FWHM) whereas at Φ = 5.4×10^{11} W/cm^2 and Φ = 7.6×10^{10} W/cm^2 the emission lasts for only 4 ns and 2.5 ns respectively (shorter than the laser pulse duration) due to the lower electron temperature achieved in the plasma generation.

ACKNOWLEDGMENT

This work was supported by Science Foundation Ireland under grant number 07/IN.1/I1771. We also thank to Dr. Larissa Juschkin and Dr. Fergal O'Reily for the very useful discussion. Technical assistance by Dave Cooney, Frank Heffernan, Victor Litera, Brian O'Connor as well as Brian Redmond is gratefully acknowledged.

REFERENCES

1. S.S. Churilov, R.R. Kildiyarova, A.N. Ryabtsev *et al*., Phys. Scr. **80**, 045303 (2009).
2. D. Kilbane and G. O'Sullivan, J. Appl. Phys. **108**, 104905 (2010).
3. T. Otsuka, D. Kilbane, J. White *et al*., Appl. Phys. Lett. **97**, 111503 (2010).
4. T. Otsuka, D. Kilbane, T. Higashiguchi *et al*., Appl. Phys. Lett. **97**, 231503 (2010).
5. K. Koshelev, V. Krivtsun, R. Gayasov *et al*., *Experimental Study of Laser Produced gadolinium Plasma Emitting at 6.7 nm*, Proceedings of the 2010 International Workshop on EUV Sources (2010) 20.
6. V. Banine, A. Yakunin and D. Glushkov, *Next Generation of EUV Lithography: Challenges and Opportunities*, Proceedings of the 2010 International Workshop on EUV Sources, (2010) 14.
7. I.A. Makhotkin, E. Zoethout, E. Louis *et al*., J. Micro/Nanolith. MEMS MOEMS **11** 040501 (2012).
8. J. Benschop, *EUV: Status and Challenges Ahead*, Proceedings of the 2010 International Workshop on EUVL (2010) 1.
9. T. Otsuka, D. Kilbane, J. White *et al*., Appl. Phys. Lett. **97**, 111503 (2010).
10. T. Otsuka, D. Kilbane, T. Higashiguchi, *et al*., Appl. Phys. Lett. **97**, 231503 (2010).
11. T. Cummins, T. Otsuka, N. Yugami, *et al*., Appl. Phys. Lett. **100**, 061118 (2012).
12. C.O'Gorman, T. Otsuka, N. Yugami *et al*., Appl. Phys. Lett. **100**, 141108 (2012).
13. S.S. Churilov, R.R. Kildiyarova, A.N. Ryabtsev, *et al.*, Phys. Scr. **80**, 045303 (2009).
14. G.O'Sullivan and B. Li, J. Micro/Nanolith. MEMS MEOMS **11**, 021108 (2012).
15. B. Li, P. Dunne, T. Higashiguchi, T. Otsuka *et al*., Appl. Phys. Lett. **99**, 231502 (2011).
16. D. Kilbane and G. O'Sullivan, J. Appl. Phys. **108**, 104905 (2010).
17. O. Morris, F. O'Reilly, P. Dunne, *et al*., Appl. Phys. Lett. **92**, 231503 (2008).
18. J. Filevich, J.J. Rocca, E. Jankowska *et al*., Phys. Rev. E **67**, 056409 (2003).
19. R.D. Cowan, The Theory of Atomic Structure and Spectra, Berkeley University of California Press, Berkeley (1981) 5.